Adaptive Sliding-Window Coded Modulation in Cellular Networks

Kwang Taik Kim*, Seok-Ki Ahn*, Young-Han Kim†, Hosung Park‡
Lele Wang†, Chiao-Yi Chen†, Jeongho Park*
*Digital Media & Communications Research Center, Samsung Electronics, Suwon, Gyeonggi-do 443-742, Korea
Email: {kwangtaik.kim, seokki.ahn, jeongho.jh.park}@samsung.com
†Department of Electrical and Computer Engineering, University of California, San Diego, La Jolla, CA 92093
Email: {yhk, lew001, chc111}@ucsd.edu
‡School of Electronics & Computer Engineering, Chonnam National University, Gwangju 500-757, Korea
Email: hpark1@chonnam.ac.kr

***Abstract*—The sliding-window superposition coding scheme aims to mitigate intercell interference at the physical layer by achieving the simultaneous decoding performance with point-to-point channel codes, low-complexity decoding, and minimal coordination overhead. The associated sliding-window coded modulation (SWCM) scheme can be readily implemented using standard off-the-shelf codes, such as the standard LTE turbo code, and tracks the information-theoretical performance guarantee of sliding-window superposition coding. This paper investigates how the basic SWCM scheme performs for the Ped-B fading interference channel model and proposes several improvements in transceiver design, such as soft decoding, input bit-mapping and layer optimization, and power control. Our enhanced SWCM scheme achieves the rates higher than those of the basic SWCM scheme by 10% to 20%, which already shows a significant gain over existing schemes that ignore modulation or coding information of interfering signals. This result confirms the potential of SWCM as a basic building block for physical-layer interference management in 5G and subsequent generations of cellular networks.**

I. Introduction

The fifth-generation (5G) cellular networks, spurred by the need for a more efficient utilization of existing and mmWave frequencies, are expected to deploy cells more densely than 4G networks. Consequently, co-channel interference would likely become one of the major performance bottlenecks to achieve high cell throughput [1]. Smart co-channel interference management schemes in the physical (PHY) layer thus would become one of key enabling technologies for 5G, provided that they can offer high spectral efficiency, avoid data sharing or heavy coordination overhead on the network side, and maintain computational complexity comparable to techniques widely used in point-to-point (p2p) communication.

Most existing communication systems either avoid interference using orthogonal time/frequency resources or treat interference as (Gaussian) noise (IAN). Both schemes are simple and can utilize existing p2p coding techniques. Exploiting the modulation information of interfering signals, IAN can be enhanced to the interference-aware detection (IAD) scheme [2], the signaling and network-side operations of which are now standardized in recently completed Third-Generation Partnership Project (3GPP) Release 12 [3]. Both IAN and IAD achieve fairly good performance when interference is weak, but their performance degrades as interference becomes stronger.

Information theory shows that in order to achieve better performance, receivers are required to decode for both the desired signal and part or whole of the interfering signal, often referred as simultaneous nonunique decoding (SND) [4]. In fact, SND achieves the optimal maximum likelihood decoding performance when the senders use p2p random code ensembles [5], [6], [7]. As a main drawback, each receiver in SND has to employ some form of multiuser sequence detection, which is difficult to implement based on existing coding techniques.

A few approaches have been proposed to tackle this issue. First, instead of conventional p2p codes such as low-density parity check (LDPC) and turbo codes, one can use novel error-correcting codes such as spatially coupled codes [8] and polar codes [9], which can be further extended to simultaneous nonunique decoding of desired as well as interfering codewords [10], [11]. The resulting codes, however, are often of very long block lengths, not suitable to typical wireless applications. Second, interference-aware successive decoding (IASD) [12] aims to achieve the simultaneous decoding performance of turbo codes by iteratively decoding for both desired and interfering codewords. Despite the name, the scheme is not successive in the usual sense, and it performs well in general and better than successive interference cancellation schemes in particular. The scheme, however, still falls short of achieving the SND performance, especially, under moderate interference.

Recently, sliding-window superposition coding (SWSC) was proposed [13] that achieves the SND performance with p2p codes. This scheme is built on basic components of network information theory, carefully combining the ideas of block Markov coding and sliding-window decoding (commonly used for multihop relaying and feedback communication), and superposition coding without rate splitting and successive cancellation decoding (allowing low complexity decoding). This conceptual coding scheme can be turned into an implementable coded modulation scheme, whereby conventional binary codes are mapped to transmitted symbols in staggered

978-1-4799-5952-5/15/$31.00 ©2015 IEEE

layering and recovered successively at the receivers. In [14], a basic form of this sliding-window coded modulation (SWCM) scheme was studied using long-term evolution (LTE) turbo codes [15] and simple bit-mapping rules, and was shown to track the SND performance for two-user-pair Gaussian interference channels with significant performance gain over IAN and IAD.

The goal of this paper is twofold. First, we present a more extensive study on the performance of SWCM for Gaussian fading interference channels, which may serve as a feasibility test for its adoption in practice. In particular, we show how SWCM can be utilized under typical LTE standard resource allocation scenarios and how much performance improvement can be made under typical fading environments, say, Ped-B [16]. Second, we propose several enhancements to the basic SWCM scheme. On the receiver side, successive cancellation decoding can utilize soft information, which ultimately leads to a fairly general class of sliding-window iterative decoding algorithms. This enhancement boosts achievable rates in general and provides some robustness in code rate selection to satisfy desired quality of service (QoS) requirements. On the sender side, we can consider various combinations of bit-mapping rules, layering structures, and power allocation. When properly adapted to available channel quality information (CQI), these modifications bring in additional performance gain.

Throughout the paper, our focus will be on interference channels with two user-pairs, which we view as a good proxy for cellular communication scenarios with one dominant interferer at each receiver; see Fig. 1. The rest of the paper is organized as follows. In Section II, we describe the system model, including the physical channel and time/frequency resource allocation models. Section III recalls the basic SWCM scheme. The main contributions of the paper appear in Sections IV (receiver-side enhancements) and V (sender-side enhancements). In Section VI, we evaluate the overall performance of the combined adaptive transmitter and receiver techniques, and compare it with the performance of basic SWCM, IASD, IAD, IAN, and interference-free. Our enhanced SWCM scheme universally outperforms all existing schemes over all SNRs and INRs.

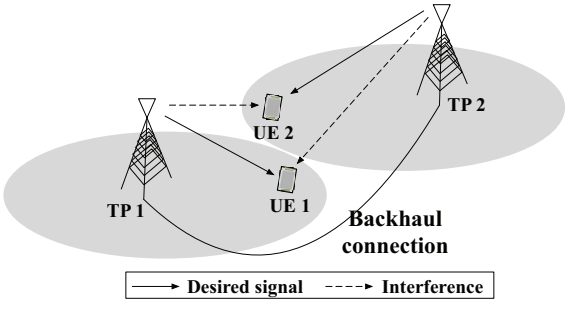

Fig. 1: Interference-limited cellular network with one dominant interference.

II. System Model

A. Gaussian Interference Channel with Two User-Pairs

As a simple model for wireless communication systems with one dominant interferer in the same time and frequency, we consider the two-user-pair Gaussian interference channel [4]. The outputs of the channel corresponding to the inputs X_1 and X_2 are

$$\begin{aligned} Y_1 &= G_{11}X_1 + G_{12}X_2 + Z_1, \\ Y_2 &= G_{21}X_1 + G_{22}X_2 + Z_2, \end{aligned} \tag{1}$$

where G_{ij}, $i, j = 1, 2$, is the channel gain from sender j to receiver i, and $Z_1 \sim \mathrm{N}(0, N_0/2)$ and $Z_2 \sim \mathrm{N}(0, N_0/2)$ are additive white Gaussian noise components. We assume without loss of generality that $N_0/2 = 1$. We also assume average power constraint P on X_i, $i = 1, 2$, and define received signal-to-noise ratios (SNRs) as $\mathrm{SNR}_1 = G_{11}^2 P$, $\mathrm{SNR}_2 = G_{22}^2 P$ and received interference-to-noise ratios (INRs) as $\mathrm{INR}_1 = G_{12}^2 P$, $\mathrm{INR}_2 = G_{21}^2 P$.

We consider two scenarios on the channel gains G_{ij}. For exposition of basic concepts, we assume that G_{ij} is constant during transmission (no fading). For performance simulations, we assume that G_{ij} is randomly drawn according to the Ped-B model [16] under the time/frequency structure explained in the next subsection. In both scenarios, receiver $i = 1, 2$ is assumed to have complete knowledge of G_{i1} and G_{i2}.

B. Frame Structure and Resource Allocation

We assume that communication over the interference channel model (1) follows the 3GPP LTE standard subframe structure [17]. We allocate each transmission block 13200 resource elements (REs) by subtracting physical downlink control channel (PDCCH) REs from 100 resource blocks (RBs) in a subframe. Thus, codewords are transmitted by 13200 PAM symbols. Ped-B channel gains for an OFDM symbol of the subframe over 2048 subcarriers are obtained by taking a fast Fourier transform (FFT) of 6 Rayleigh distributed multipath channel taps [16]. We use the Jakes model [18] for time correlation of the channel gains due to pedestrian mobility (3 km/h in the Ped-B channel) between OFDM symbols of 32.5 ns duration, and define the average SNR (or INR) as the average received power of the sum of 6 multipath signals. The channel gains for all four links in (1) are generated by applying this process independently. We finally map virtual REs to physical REs by pseudorandom interleaving for frequency diversity. Because the maximum size of the quadratic permutation polynomial (QPP) interleaver of the LTE standard turbo code [15] is 6144, we divide the transmission block into a few segmented *subblocks* (for the case of IAN, IAD, and IASD), when code rates are high. SWCM has a natural subblock structure. In this paper, we divide the block of 13200 PAM symbols into 20 subblocks each consisting of 660 symbols, well within the range of the QPP interleaver.

III. Basic Sliding-Window Coded Modulation

Given a random code ensemble with input pmfs $p(x_1)$ and $p(x_2)$, the achievable rate region under the optimal maximum likelihood decoding rule can be characterized [7] as the intersection of $\mathscr{R}_1$ and $\mathscr{R}_2$, where $\mathscr{R}_1$ is the set of rate pairs (R_1, R_2) such that

$$R_1 \le I(X_1; Y_1)$$

or

$$\begin{aligned} R_1 &\le I(X_1; Y_1|X_2), \\ R_1 + R_2 &\le \min\{I(X_1, X_2; Y_1), I(X_1, X_2; Y_2)\}, \end{aligned}$$

and $\mathscr{R}_2$ is defined similarly with subscripts $1 \leftrightarrow 2$. This rate region can be achieved by simultaneous nonunique decoding (SND) at the receivers.

As a low-complexity alternative, the sliding-window superposition coding (SWSC) scheme has been proposed [13], whereby senders transmit codewords over multiple subblocks and multiple superimposed layers in a staggered manner and receivers recover desired as well as interfering codewords over a sliding-window of subblocks by successive cancellation decoding. Noting the fact that PAM or QAM signals can be represented as superposition of PAM or QAM signals of smaller constellation sizes, we can specialize the general SWSC scheme to be compatible with existing binary block codes. In the following, we describe a basic form of this sliding-window coded modulation (SWCM) scheme [14], which we will use as our baseline in this paper.

We consider b transmission subblocks, each consisting of n transmissions. A sequence of $(b-1)$ messages $m_1(j) \in [1, 2, \cdots, 2^{nR_1}]$ carried by signals $V(j)$ and $U(j+1)$, $j \in [1 : b-1]$, and that of b messages $m_2(j) \in [1, 2, \cdots, 2^{nR_2}]$ carried by $W(j)$, $j \in [1 : b]$, from senders 1 and 2, respectively, are to be sent over the two-user-pair Gaussian interference channel in nb transmissions. Note that dummy messages $m_1(0) = m_1(b) = 1$ are carried by $U(1)$ and $V(b)$ separately. For practical implementation of basic SWCM with p2p channel codes, we use a binary linear LTE standard turbo code [15] of length $2n$ and rate $R_1/2$ to form signal $[V(j-1)|U(j)]$ carrying $m_1(j-1)$ via encoding $m_1(j-1)$ into codeword $c_1(j-1)$ of length $2n$, scrambling $c_1(j-1)$ into $\tilde{c}_1(j-1)$, and then applying binary phase shift keying (BPSK) to $\tilde{c}_1(j-1)$, as shown in Fig. 2. The transmitted signal $X_1(j)$ is formed by superimposing signal $U(j)$ on signal $V(j)$ in the symbol-level with power allocation parameter α subject to the constraint on the transmitted power P. Similarly, a binary linear turbo code of length n and rate R_2 is used to form signal $W(j)$ carrying $m_2(j)$ via encoding $m_2(j)$ into codeword $c_2(j)$ of length n, scrambling $c_2(j)$ into $\tilde{c}_2(j)$, and then applying a standard 4-PAM to $\tilde{c}_2(j)$. The transmitted signal $X_2(j)$ is amplified according to the constraint on the transmitted power P as follows:

$$\begin{aligned} X_1(j) &= \sqrt{\alpha P}\, U(j) + \sqrt{(1-\alpha)P}\, V(j), \\ X_2(j) &= \sqrt{P}\, W(j), \end{aligned}$$

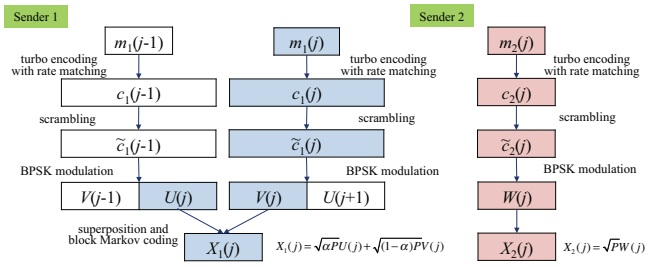

Fig. 2: The implemented procedures at senders for basic SWCM

where $U(j)$, $V(j) \in \{-1, +1\}^n$ and $W(j) \in \{-\frac{3}{\sqrt{5}}, -\frac{1}{\sqrt{5}}, +\frac{1}{\sqrt{5}}, +\frac{3}{\sqrt{5}}\}^n$. We set the power allocation parameter $\alpha = 0.8$ for standard 4-PAM signal $X_1(j)$. In this paper, we set $b = 20$ and $n = 660$ as the total blocklength is 13200; see Subsection II-B.

The outputs of the channel are

$$\begin{aligned} Y_1(j) &= g_{11}\sqrt{\alpha P}\, U(j) + g_{11}\sqrt{(1-\alpha)P}\, V(j) \\ &\quad + g_{12}\sqrt{P}\, W(j) + Z_1(j), \\ Y_2(j) &= g_{21}\sqrt{\alpha P}\, U(j) + g_{21}\sqrt{(1-\alpha)P}\, V(j) \\ &\quad + g_{22}\sqrt{P}\, W(j) + Z_2(j). \end{aligned}$$

The receivers recover messages by using sliding-window decoding and successive cancellation decoding; see Fig. 3. Receiver 1 first attempts to recover $\hat{m}_1(j-1)$ carried by signals $V(j-1)$ and $U(j)$ by decoding received signals $Y_1(j-1)$ and $Y_1(j)$ via canceling previously decoded signals $U(j-1)$ and $W(j-1)$ from $Y_1(j-1)$ and treating interfering signals $V(j)$ and $W(j)$ as noise. This phase 1 decoding step is successful if $R_1 \le I(U; Y_1) + I(V; Y_1|U, W)$. It then attempts to recover $\hat{m}_2(j)$ carried by $W(j)$ by decoding $Y_1(j)$ via canceling previously decoded signal $U(j)$ from $Y_1(j)$ and treating interfering signal $V(j)$ as noise. This phase 2 decoding step is successful if $R_2 \le I(W; Y_1|U)$. Similarly, Receiver 2 first attempts to recover $\hat{m}_1(j-1)$ carried by $V(j-1)$ and $U(j)$ by decoding received signals $Y_2(j-1)$ and $Y_2(j)$ via canceling previously decoded signal $U(j-1)$ from $Y_2(j-1)$ and treating interfering signals $W(j-1)$, $V(j)$ and $W(j)$ as noise. This phase 1 decoding step is successful if $R_1 \le I(U, V; Y_2)$. It then attempts to recover $\hat{m}_2(j-1)$ carried by $W(j-1)$ by decoding $Y_2(j-1)$ via canceling previously decoded signals $U(j-1)$ and $V(j-1)$ from $Y_2(j-1)$. This phase 2 decoding step is successful if $R_2 \le I(W; Y_2|U, V)$. Thus the achievable rate region is characterized by

$$\begin{aligned} R_1 &\le \min\{I(U; Y_1) + I(V; Y_1|U, W), I(U, V; Y_2)\}, \\ R_2 &\le \min\{I(W; Y_1|U), I(W; Y_2|U, V)\}. \end{aligned}$$

Note that different rate regions can be achieved by choosing alternative decoding orders at each receiver, which can be adapted to given channel parameters.

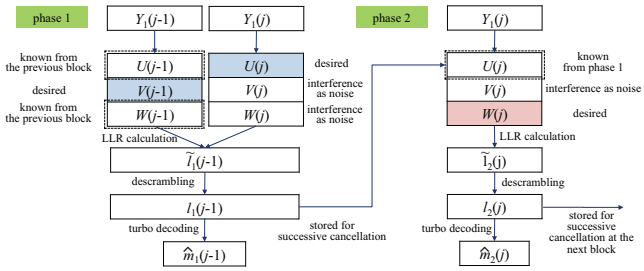

Fig. 3: Decoding order operation example. In the basic successive cancellation hard bit decoding scheme, the codeword recovered in each phase is stored and cancelled at the next phase/subblock. In the soft decoding scheme, soft information (LLR) of the codeword is stored instead and incorporated to the LLR calculation of another codeword at the next phase/subblock.

IV. Adaptive Receiver Designs

A. Successive Cancellation with Soft Information

In the basic SWCM scheme discussed in the previous section, "hard" information was used in each stage of successive cancellation decoding. As the first step to designing receivers that achieve higher throughput and reliability, we incorporate "soft" information in successive cancellation decoding. In particular, each stage of successive cancellation decoding stores log-likelihood ratios (LLRs) of the codeword of the stage, which can then be incorporated in the next stage to calculate LLRs of the new codeword; see Fig. 3.

B. Sliding-Window Iterative Decoding

The basic SWCM receiver can be further enhanced by incorporating iterative decoding instead of successive cancellation decoding. We first give a general description of the proposed sliding-window iterative soft-decision decoding:

Algorithm *Sliding-window iterative decoding*

1. **repeat**
2. Choose a certain window of subblocks
3. Choose a certain subset of messages whose transmissions are completed within the window
4. Perform iterative soft-decision decoding for the selected messages according to a certain decoding order
5. Slide the window by a certain number of subblocks
6. **until** Certain decoding completion criteria are achieved (or the process fails)

This general description can crystallize into various specific decoding operations. An interesting example is iterative decoding throughout the entire block (subblocks 1 through b). This *block iterative decoding* method helps better track the sum-rate bound achieved by simultaneous decoding. Note that both IASD and our iterative decoding algorithm perform iterative soft-decision decoding between interfering and desired signals in turn but do so at a different scale (subblock vs. block).

We demonstrate the benefit of iterative decoding via a simple Gaussian interference example with $\text{SNR}_1 = 13$ dB, $\text{INR}_1 = 7$ dB, $\text{INR}_2 = 8.5$ dB, and $\text{SNR}_2 = 13.5$ dB (this channel will be used as a running example for the rest of the paper). Here we use the same basic SWCM encoder structure described in the previous section and compare basic sliding-window successive cancellation hard-decision decoding with iterative soft-decision decoding over the entire block. As illustrated in Fig. 4, the enhanced decoder outperforms the basic decoder by 6.4% in the symmetric rate under the same 16 iterations total over desired and interfering codewords per subblock.

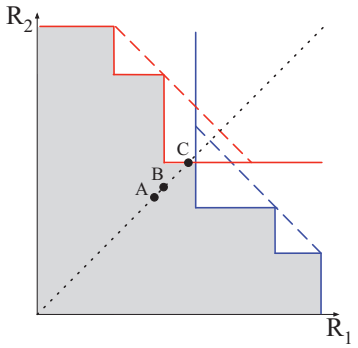

Fig. 4: Achievable symmetric rate pairs for the Gaussian interference channel under basic sliding-window successive cancellation hard-decision decoding (point A: 0.78), iterative soft-decision decoding over the block (point B: 0.83), and the theoretical limit (point C: 1.0). The dotted diagonal lines reflect the optimal SND rate region from rate conditions for each receiver. The performance in this and subsequent plots reflect error propagation and rate loss from diagonal transmission.

We now consider the symmetric Ped-B interference channel with average SNR $= 10$ dB and average INR $= 7,\ 10,\ 13$ dB. Again we fix the same basic 2/1-layer SWCM encoder structure in the previous section and compare its symmetric-rate performances under different decoding algorithms with those of IASD, IAD, and IAN. The receiver of each scheme is simulated with 16 iterations per subblock. The block length of SWCM (spanning over multiple subblocks) is matched to that of IASD, IAD, and IAN. As shown in Fig. 5, simulation results for the achievable sum-rates under symmetric QoS with BLER $= 0.1$ (subblock error rate is abbreviated to BLER in this paper) demonstrate that the SWCM scheme with the proposed iterative decoding algorithm outperforms the basic SWCM scheme, IASD, IAD, and IAN uniformly for all INRs. For example, SWCM with iterative decoding outperforms basic SWCM by 9.6% and IASD by 10.5% at INR $= 10$ dB.

V. Adaptive Transmitter Designs

The basic SWCM scheme cannot achieve every rate pair achievable by simultaneous decoding due to structural constraints imposed by modulation. The auxiliary inputs U, V, W

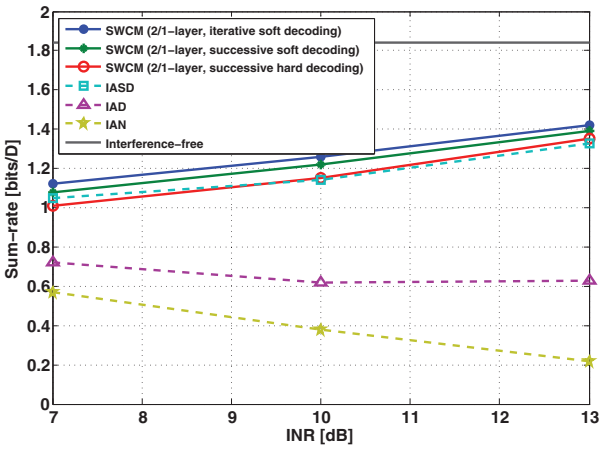

Fig. 5: Achievable sum-rates under the symmetric rate QoS for the 2/1-layer SWCM scheme with iterative soft decoding, the 2/1-layer SWCM scheme with successive soft decoding, the 2/1-layer SWCM scheme with successive hard decoding (basic SWCM), IASD, IAD, and IAN at BLER $= 0.1$ plotted vs average received INR in the symmetric Ped-B interference channel with average received SNR = 10 dB.

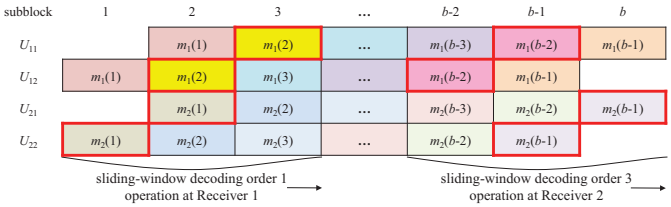

Fig. 6: The encoding and decoding operations of the 2/2-layer SWCM scheme for b subblocks.

introduced in Section III should be PAM signals, which leads to the staircase shape of achievable regions instead of typical pentagonal regions; see Fig. 4. We propose three enhancements to the basic SWCM encoding structure.

A. Multiple Layers for Both Senders

Using two signal layers for both senders, referred to as the *2/2-layer SWCM scheme* (see Fig. 6 for its encoding and decoding operations), can potentially enlarge the SWCM achievable rate region. As illustrated in Fig. 4, the basic 2/1-layer SWCM scheme fails to achieve the SND performance under the symmetric rate QoS requirement. However, the achievable rate region of the 2/2-layer SWCM scheme has more staircase steps (in general, the more the layers, the more the steps) and thus can approach the diagonal part of the SND region better. As shown in Figures 4 and 7, the 2/2-layer scheme (point D) outperforms the basic 2/1-layer scheme (point A in Fig. 4) by 5.1% in the symmetric rate under the same 16 iterations.

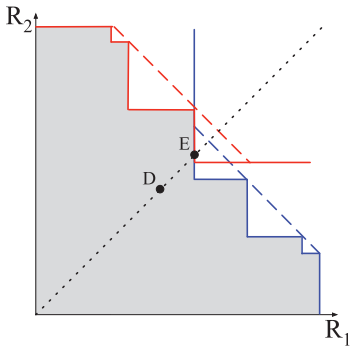

Fig. 7: Achievable symmetric rate pairs for the same channel as in Fig. 4 under 2/2-layer SWCM with successive hard decision decoding (point D: 0.82), and the theoretical limit (point E: 1.06).

B. Adaptive Bit Mapping

Different combinations of various bit mapping rules at both senders can be adaptively chosen to enlarge the SWCM achievable rate region. There are several bit mapping rules for the structure of auxiliary inputs for superposition coding. For example, the 2/2-layer SWCM scheme has the following three bit mapping rules for each sender $i = 1, 2$:

1) $X_i(j) = \sqrt{\alpha_i \bar{P}}\, U_{i1}(j) + \sqrt{(1-\alpha_i)\bar{P}}\, U_{i2}(j)$
2) $X_i(j) = \sqrt{(1-\alpha_i)\bar{P}}\, U_{i1}(j) + \sqrt{\alpha_i \bar{P}}\, U_{i2}(j)$
3) $X_i(j) = \sqrt{\alpha_i \bar{P}}\, U_{i1}(j) + \sqrt{(1-\alpha_i)\bar{P}}\, U_{i1}(j) U_{i2}(j)$

for $j \in [1 : b]$. There are total nine combinations of bit mapping rules for 2/2-layer SWCM. Each combination of bit mapping rules characterizes a different achievable rate region. In particular, the achievable rate region with bit mapping rules 1 and 2 with $\alpha_1 = \alpha_2 = 0.8$ at senders 1 and 2, respectively, can achieve higher sum-rates than can be achieved by the natural bit mapping rule, as illustrated in Fig. 8. The enhanced encoder using adaptive bit mapping (point F) outperforms the enhanced encoder using natural bit mapping (point D in Fig. 7) by 7.3% in the symmetric rate under the same 16 iterations.

C. Power Allocation

We can adaptively choose power allocation parameters between superimposed layers, for example, $\alpha_i \in [0, 1]$ in 2-layer superimposed signal $X_i(j) = \sqrt{\alpha_i \bar{P}}\, U_{i1}(j) + \sqrt{(1-\alpha_i)\bar{P}}\, U_{i2}(j)$. With varying power allocation parameters, modulated symbols change (for example, *uniform* 4-PAM X_i corresponds to $\alpha_i = 0.8$), which in turn change the corresponding SND rate region as well as the SWCM achievable rate region (as the latter is the staircase approximation of the SND region). For brevity, we omit feasibility plots demonstrating the effect of power allocation.

D. Performance of Adaptive Transmitters in the Ped-B Interference Channel

We again consider the symmetric Ped-B interference channel with average SNR $= 10$ dB and INR $= 7,\ 10,\ 13$ dB.

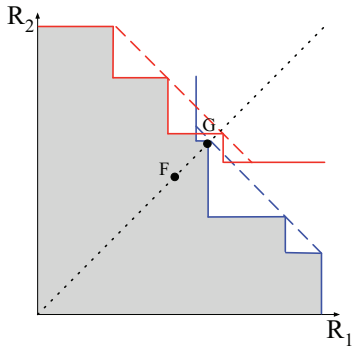

Fig. 8: Achievable symmetric rate pairs for the same channel as in Fig. 4 under 2/2-layer SWCM with bit mapping rule optimization and successive hard decision decoding (point F: 0.88), and the theoretical limit (point G: 1.13).

Here we use the basic SWCM decoder structure (successive hard-decision decoding) described in Section III and compare its symmetric-rate performances under different encoding algorithms with those of IASD, IAD, and IAN. The receiver of each scheme is simulated with 16 iterations per subblock. The block length of SWCM is matched to that of IASD, IAD, and IAN. As shown in Fig. 9, simulation results for the achievable sum-rates under symmetric QoS with BLER $= 0.1$ demonstrate that the 2/2-layer SWCM scheme with the proposed adaptive bit mapping algorithm outperforms the basic SWCM scheme, IASD, IAD, and IAN uniformly for all INRs. For example, 2/2-layer SWCM with adaptive bit mapping outperforms basic SWCM by 16.5% and IASD by 17.5% at INR $= 10$ dB.

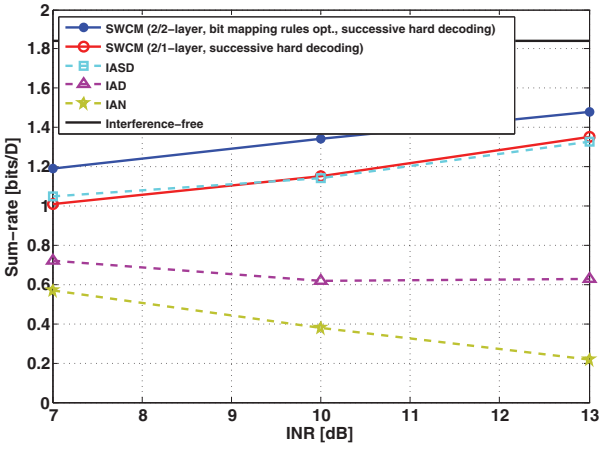

Fig. 9: Achievable sum-rates under the symmetric rate QoS for the 2/2-layer SWCM scheme with bit mapping rules optimization for each subframe and successive hard decoding, the 2/1-layer SWCM scheme with successive hard decoding (Basic SWCM), IASD, IAD, and IAN at BLER $= 0.1$ plotted vs average received INR in the symmetric Ped-B interference channel with average received SNR = 10 dB.

Note that 2/2-layer SWCM with adaptive bit mapping and successive hard decoding, which enhances only the encoding operation, outperforms even 2/1-layer SWCM with iterative soft decoding (see Fig. 5), which enhances only the *decoding* operation, uniformly for all INRs. This implies that using SWCM at both senders and choosing right mapping rules adaptively for required rate pairs play a more crucial role for high performance, unless available CQI feedback at senders is outdated. In case the CQI feedback is outdated, the adaptive receivers proposed in the previous section would remedy the performance loss due to the mismatch.

VI. Simulation Results of Combined Adaptive Transmitter and Receiver Techniques

We evaluate the overall performance of the combined adaptive transmitter and receiver techniques enhancing the basic SWCM scheme in the Ped-B interference channel. We consider three symmetric Ped-B interference channels with 1) average SNR $= 10$ dB and INR $= 7,\ 10,\ 13$ dB; 2) average INR $= 10$ dB and SNR $= 7,\ 10,\ 13$ dB; and 3) average SNR $=$ INR $= 7,\ 10,\ 13$ dB. We assume the symmetric rate QoS requirement at the receivers. The receiver of each scheme is simulated with 16 iterations total per subblock. The block length of SWCM is matched to that of IASD, IAD, and IAN.

Simulation results for the achievable sum-rates with BLER $= 0.1$ demonstrate that the enhanced SWCM scheme with combined adaptive transmitter and receiver techniques outperforms the basic SWCM scheme, IASD, IAD, and IAN uniformly for all SNRs and INRs, as shown in Figures 10–12. For example, the enhanced SWCM scheme outperforms basic SWCM by 11.4–21.8% and IASD by 14.3–19.6%. In particular, the enhanced SWCM scheme achieves a large performance gap from the achievable sum-rate of IASD for

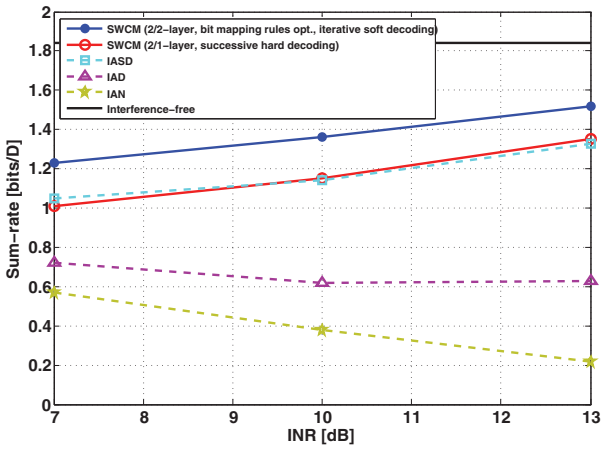

Fig. 10: Achievable sum-rates under the symmetric rate QoS for the basic and enhanced SWCM schemes, IASD, IAD, and IAN at BLER $= 0.1$ plotted vs average received INR in the symmetric Ped-B interference channel with average received SNR = 10 dB.

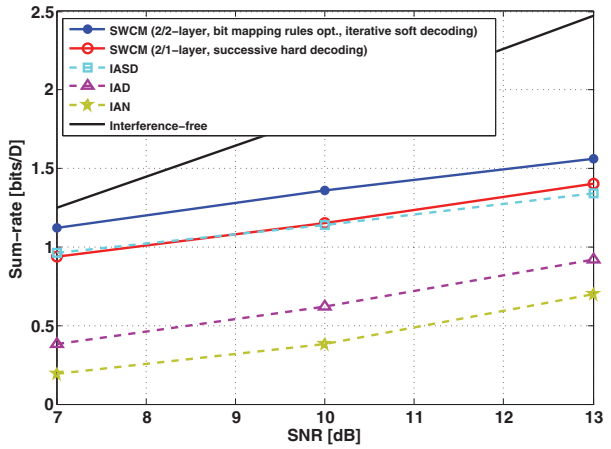

Fig. 11: Achievable sum-rates under the symmetric rate QoS for the basic and enhanced SWCM schemes, IASD, IAD, and IAN at BLER $= 0.1$ plotted vs average received INR in the symmetric Ped-B interference channel with average received INR = 10 dB.

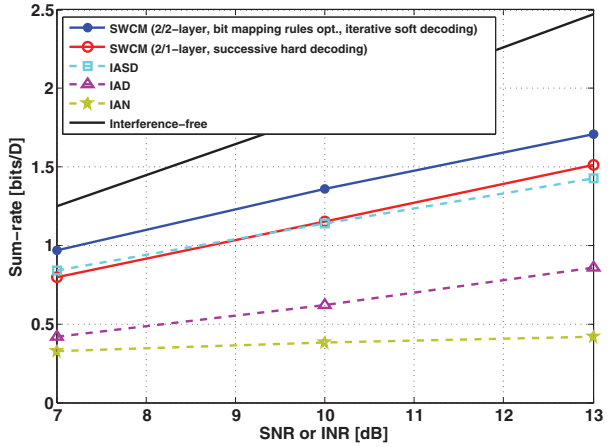

Fig. 12: Achievable sum-rates under the symmetric rate QoS for the basic and enhanced SWCM schemes, IASD, IAD, and IAN at BLER $= 0.1$ plotted vs average received INR in the symmetric Ped-B interference channel with average received SNR $=$ INR (signal-to-interference ratio $= 0$ dB).

SNR $=$ INR, as shown in Fig. 12. Even the basic SWCM scheme outperforms IASD by 5.6% at SNR $=$ INR $= 13$ dB.

Finally we note that neither the basic nor the enhanced SWCM scheme necessarily require much higher computational complexity. Most importantly, all our simulation results use the same number of 16 iterations. Adaptive selection of transmitter techniques and of decoding orders (which is our main contribution), just as in most adaptive transceiver designs in wireless communication systems, is nontrivial in general, but can be chosen according to lookup tables that can be computed offline and we expect that simple heuristic approaches emerge as more subsequent studies follow.

REFERENCES

[1] DMC R&D Center, Samsung Electronics Co., Ltd, "5G vision," 2015, White paper available at http://www.samsung.com/global/business/networks/insights/white-paper.

[2] J. Lee, D. Toumpakaris, and W. Yu, "Interference mitigation via joint detection," *IEEE J. Select. Areas in Commun.*, vol. 29, no. 6, pp. 1172–1184, June 2011.

[3] 3GPP TSG-RAN WG1 Meeting #78, "R1-143535: LS for Rel-12 NAICS," *Release 12*, 2014.

[4] A. El Gamal and Y.-H. Kim, *Network Information Theory*. Cambridge: Cambridge University Press, 2011.

[5] A. S. Motahari and A. K. Khandani, "To decode the interference or to consider it as noise," *IEEE Trans. Inf. Theory*, vol. 57, no. 3, pp. 1274–1283, Mar. 2011.

[6] F. Baccelli, A. El Gamal, and D. N. C. Tse, "Interference networks with point-to-point codes," *IEEE Trans. Inf. Theory*, vol. 57, no. 5, pp. 2582–2596, May 2011.

[7] B. Bandemer, A. El Gamal, and Y.-H. Kim, "Simultaneous nonunique decoding is rate-optimal," in *Proc. 50th Ann. Allerton Conf. Comm. Control Comput.*, Monticello, IL, Oct. 2012.

[8] S. Kudekar, T. J. Richardson, and R. L. Urbanke, "Threshold saturation via spatial coupling: Why convolutional ldpc ensembles perform so well over the bec," *IEEE Trans. Inf. Theory*, vol. 57, no. 2, pp. 803–834, Feb. 2011.

[9] E. Arıkan, "Channel polarization: A method for constructing capacity-achieving codes for symmetric binary-input memoryless channels," *IEEE Trans. Inf. Theory*, vol. 55, no. 7, pp. 3051–3073, Jul. 2009.

[10] A. Yedla, P. Nguyen, H. Pfister, and K. Narayanan, "Universal codes for the Gaussian MAC via spatial coupling," in *Proc. 49th Ann. Allerton Conf. Comm. Control Comput.*, Monticello, IL, Sep. 2011, pp. 1801–1808.

[11] L. Wang and E. Şaşoğlu, "Polar coding for interference networks," 2014, preprint available at http://arxiv.org/abs/1401.7293.

[12] J. Lee, H. Kwon, and I. Kang, "Interference mitigation in MIMO interference channel via successive single-user soft decoding," in *Proc. UCSD Inf. Theory Appl. Workshop*, La Jolla, CA, Feb. 2012, pp. 180–185.

[13] L. Wang, E. Şaşoğlu, and Y.-H. Kim, "Sliding-window superposition coding for interference networks," in *Proc. IEEE Int. Symp. Inf. Theory*, Honolulu, HI, Jul. 2014, pp. 2749–2753.

[14] H. Park, Y.-H. Kim, and L. Wang, "Interference management via sliding-window superposition coding," in *Proc. of the International Workshop on Emerging Technologies for 5G Wireless Cellular Networks, IEEE GLOBECOM*, Austin, TX, Dec. 2014, pp. 1057–1061.

[15] 3GPP TS 36.212, "Multiplexing and channel coding," *Release 12*, 2013.

[16] Recommendation ITU-R M.1225, "Guidelines for evaluation of radio transmission technologies for IMT-2000," *Int. Telecommun. Union*, 1997.

[17] 3GPP TS 36.211, "Physical channels and modulation," *Release 12*, 2013.

[18] W. C. Jakes, *Microwave Mobile Communications*. New York: IEEE Press, 1994.